Supporting Information: SILAC phosphoproteomics reveals unique signaling circuits in CAR T cells and the inhibition of B cell-activating phosphorylation in target cells

Alijah A. Griffith[1,¶], Kenneth P. Callahan[1,¶], Nathan Gordo King[1], Qian Xiao[2], Xiaolei Su[2], Arthur R. Salomon[*,1]

1 *Department of Molecular Biology, Cell Biology & Biochemistry, Brown University, Providence, RI, 02912*

2 *Department of Cell Biology, Yale School of Medicine, Yale University, New Haven, CT, 06520*
¶ Contributed equally to this work[*]

E-mail: art@drsalomon.com

Table Of Contents

Supplementary Table 1: (.XLSX) Complete list of peptides identified after heavy isotope labeling of Raji B cells and their labeling status.

Supplementary Table 2: (.XLSX) All peptides identified from sSH2 pTyr enrichment after coculture of CD19-CAR T cells and Raji B cells.

Supplementary Table 3: (.XLSX) All peptides identified from TiO_2 phosphopeptide enrichment after coculture of CD19-CAR T cells and Raji B cells.

Supplementary Table 4:	(.XLSX) Unique peptides identified from sSH2 pTyr enrichment after coculture of CD19-CAR T cells and Raji B cells.
Supplementary Table 5:	(.XLSX) Unique peptides identified from TiO_2 phosphopeptide enrichment after coculture of CD19-CAR T cells and Raji B cells.
Supplementary Folder 1:	(.ZIP) All Python 3 code used to run PTM-SEA, generate PTM-SEA heatmaps and perform statistics Western blots. Western blot quantification excel files are included here.
Supplementary Figure 1:	Fluorescence activated cell sorting (FACS) determines the population of Jurkat T-cells expressing the CD19 (CD28/4-1BB/CD3ζ/sGFP) CAR construct.
Supplementary Figure 2:	Cropped Western blots and quantification for cocultures with Raji B cells and CD19-CAR T cells Jurkat E6.1 cocultures.
Supplementary Figure 3:	Unropped Western blots for cocultures with Raji B cells and CD19-CAR T cells Jurkat E6.1 cocultures.
Supplementary Figure 4:	Pairwise correlation between replicate peptides from the TiO_2 phosphoenrichment dataset.
Supplementary Figure 5:	Pairwise correlation between replicate peptides from the sSH2 pTyr enrichment dataset.
Supplementary Figure 6:	(.PDF) All abundance heat maps for unique phosphopeptides identified by pTyr enrichment after coculture of CD19-CAR T cells and Raji B cells.
Supplementary Figure 7:	(.PDF) All abundance heat maps for unique phosphopeptides identified by TiO_2 phosphopeptide enrichment after coculture of CD19-CAR T cells and Raji B cells.
Supplementary Figure 8:	Venn diagram showing the overlap between significantly changing sSH2 and TiO_2 pTyr PSMs.
Supplementary Figure 9:	Full, uncropped Western blots for α-pTyr (4G10) and α-pErk for the proteomic samples.
Supplementary Figure 10:	PTM-SEA on CD19 CAR T-cell originating phosphopeptides observed in the sSH2 enrichment data.
Supplementary Figure 11:	PTM-SEA on Raji B-cell originating phosphopeptides observed in the sSH2 enrichment data.
Supplementary Figure 12:	Full, uncropped Western blots showing the abundance of Lck and total protein abundance in JE6, CD19-CAR T cells and Raji B cells.
Supplementary Figure 13:	PTM-SEA on phosphopeptides originating from Raji B cell observed in the TiO_2 enrichment data.

Supplementary Table 1: Complete list of peptides identified after heavy isotope labeling of Raji B cells and their labeling status. Included are the protein name, assigned peptide sequence, MOWSE score, mass error, SILAC labeling status, heavy proline inclusion, isolated mass, scan number, charge state, UNIPROT accesssion number, UNIPROT gene name, NCBI gi and HPRD accession number for each peptide identified. In total, we observed 5,038 heavy, 11 light and 5 mixed isotope labeled peptides after 8 doublings of Raji B cells in SILAC media.

Supplementary Table 2: All peptides identified from sSH2 pTyr enrichment after coculture of CD19-CAR T cells and Raji B cells. All LC-MS/MS data corresponding to each replicate and each condition are listed as separated worksheets. The assigned names are listed, as well as the position of phosphorylation in the assigned peptide sequence. The star character ($*$) represents a phosphorylated amino acid, the pound character (#) represents methionine oxidation, and the period characters (.) represent the ends of the identified peptide. For each peptide, the MOWSE score, mass error, SILAC labeling status, heavy proline inclusion, isolated mass, scan number, charge state, UNIPROT accesssion number, UNIPROT gene name, NCBI gi and HPRD accession number are reported.

Supplementary Table 3: All peptides identified from TiO_2 phosphopeptide enrichment after coculture of CD19-CAR T cells and Raji B cells. All LC-MS/MS data corresponding to each replicate and each condition are listed as separated worksheets. The assigned names are listed, as well as the position of phosphorylation in the assigned peptide sequence. The star character ($*$) represents a phosphorylated amino acid, the pound character (#) represents methionine oxidation, and the period characters (.) represent the ends of the identified peptide. For each peptide, the MOWSE score, mass error, SILAC labeling status, heavy proline inclusion, isolated mass, scan number, charge state, UNIPROT accesssion number, UNIPROT gene name, NCBI gi and HPRD accession number are reported.

Supplementary Table 4: Unique peptides identified from sSH2 pTyr enrichment after coculture of CD19-CAR T cells and Raji B cells. For each peptide, the SIC peak areas for each replicate measurment and time point, q-values, accession numbers and KEGG/GO annotations are provided. Phosphopeptide assignments were filtered by a MOWSE score greater than 20, forward hits only, and assigned an Ascore.

Supplementary Table 5: Unique peptides identified from TiO_2 phosphopeptide enrichment after coculture of CD19-CAR T cells and Raji B cells. For each peptide, the SIC peak areas for each replicate measurment and time point, q-values, accession numbers and KEGG/GO annotations are provided. Phosphopeptide assignments were filtered by a MOWSE score greater than 20, forward hits only, and assigned an Ascore.

Supplementary Folder 1: All Python 3 code used to run PTM-SEA, generate PTM-SEA heatmaps and perform statistics on Western blots. Included in this folder are all scripts (and helper scripts) used for PTM-SEA, KEGG/GO and Western blot graph generation, the required input files for each script, and the raw output from each script. Included in this folder are all Microsoft Excel files containing Western blot signal quantification exported from Image Studio (Version 5.2). For a more detailed description of use for these scripts, refer to the docstring of each script or our GitHub page (https://github.com/drsalomon/griffith_callahan_2021_CART_code).

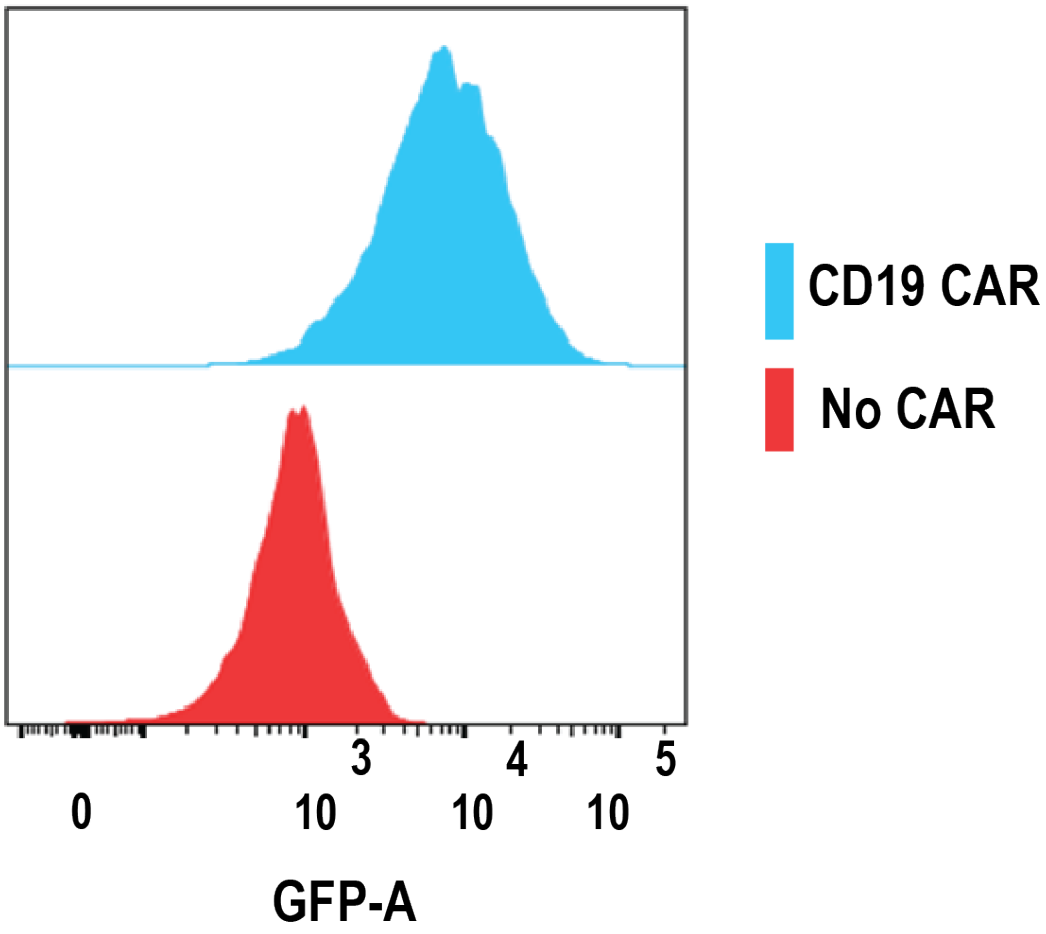

Supplementary Figure 1: Fluorescence activated cell sorting (FACS) determines the population of Jurkat T-cells expressing the CD19 (CD28/4-1BB/CD3ζ/sGFP) CAR construct.

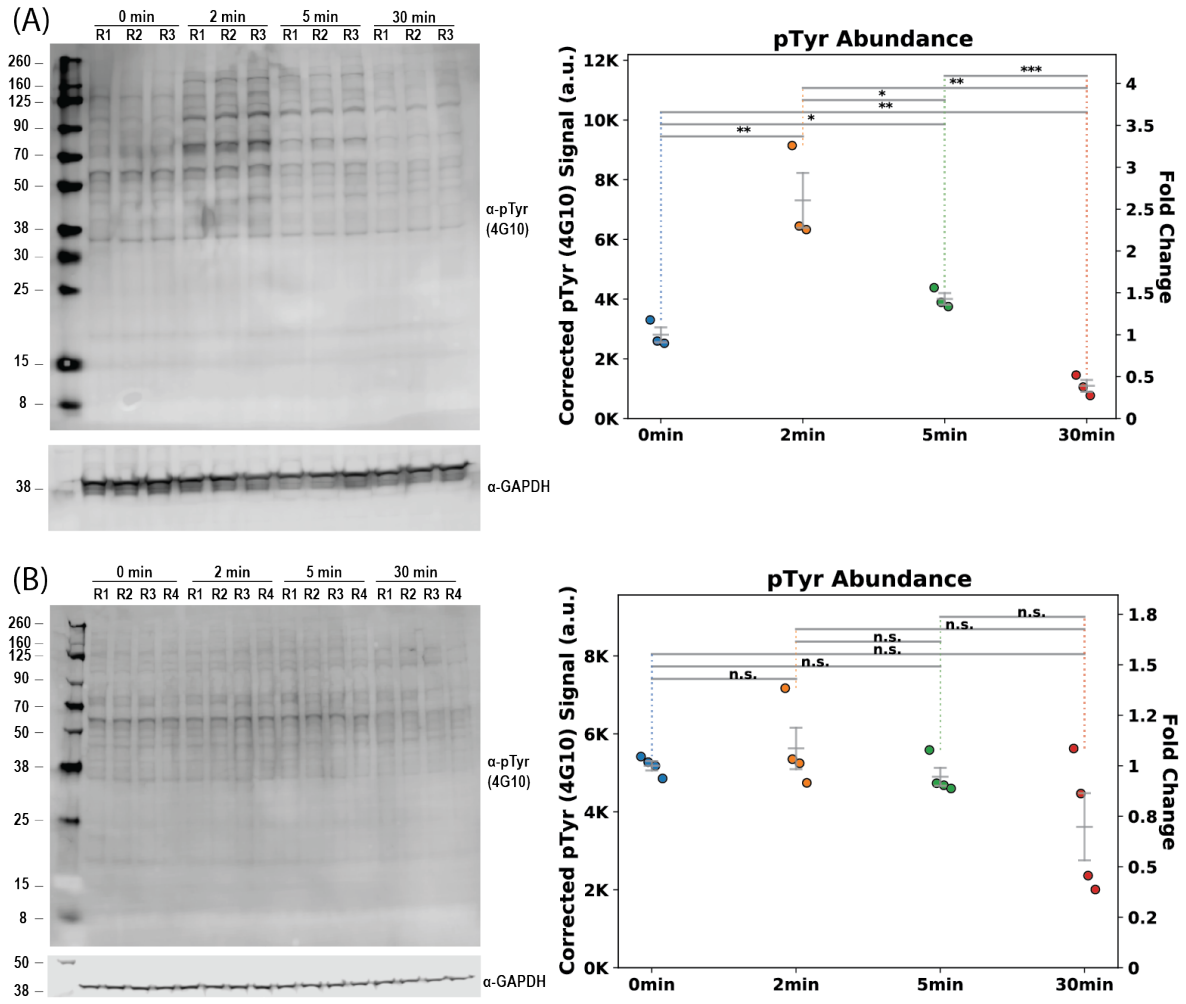

Supplementary Figure 2: Changes in pTyr abundance after coculture between Raji B cells and (A) CD19-CAR Jurkat T cells and (B) parental Jurkat E6.1 cells. For each Western blot, cropped membranes showing pTyr and GAPDH abundance and signal quantification with Fold Change relative to 0 minutes are shown. Mean corrected fluorescence intensity ± SEM are shown in grey. Stars represent statistical significance as determined by Student's T tests: "n.s." indicates $p \geq 0.05$, $*$ indicates $p < 0.05$, $**$ indicates $p < 0.01$ and $***$ indicates $p < 0.001$.

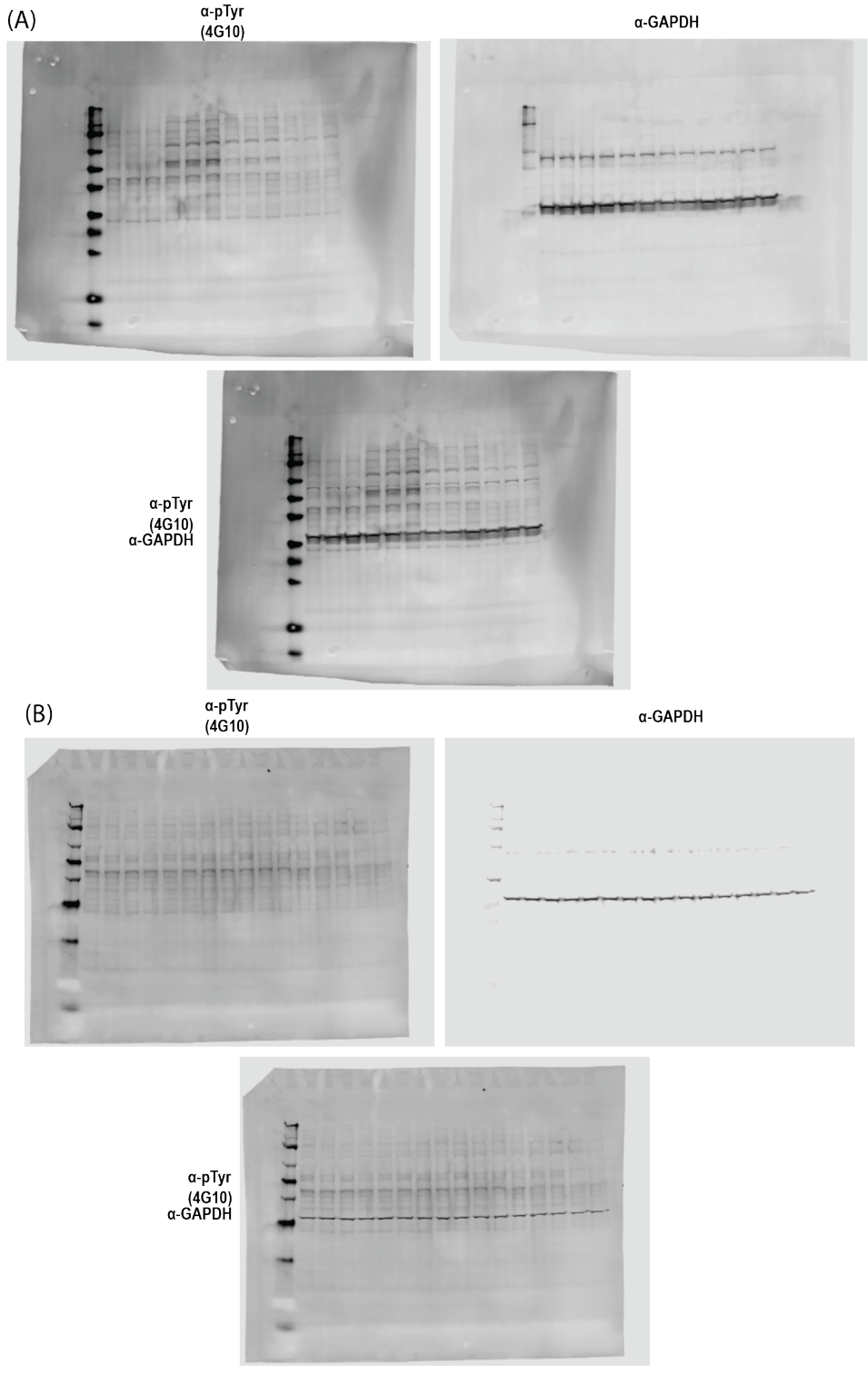

Supplementary Figure 3: Full, uncropped Western blots for coculture between Raji B cells and (A) CD19-CAR Jurkat T cells and (B) parental Jurkat cells.

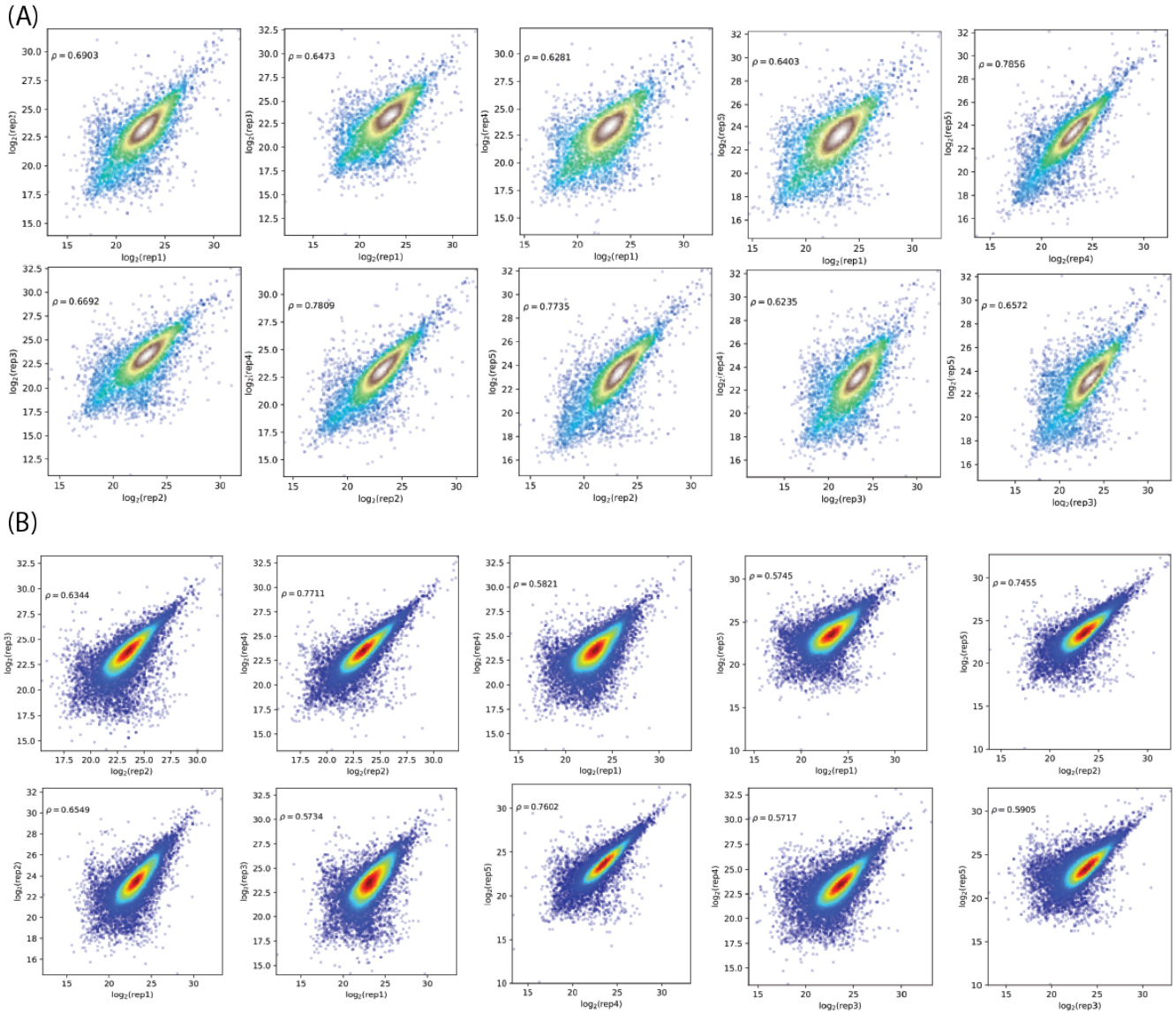

Supplementary Figure 4: Pairwise comparisons between replicates of $\log_2$ transformed phosphopeptide abundances with the same assigned sequence and charge state obtained by TiO_2 phosphoenrichment. (A) Phosphopeptide abundances measured from $CD19^{HI}$ Raji B-cells and (B) Phosphopeptide abundances measured from CD19 CAR T-cells. For each comparison, we used the Pearson's correlation coefficient (denoted ρ) as an estimate of the linear correlation between replicates and thus a measure of reproducibility between replicates.

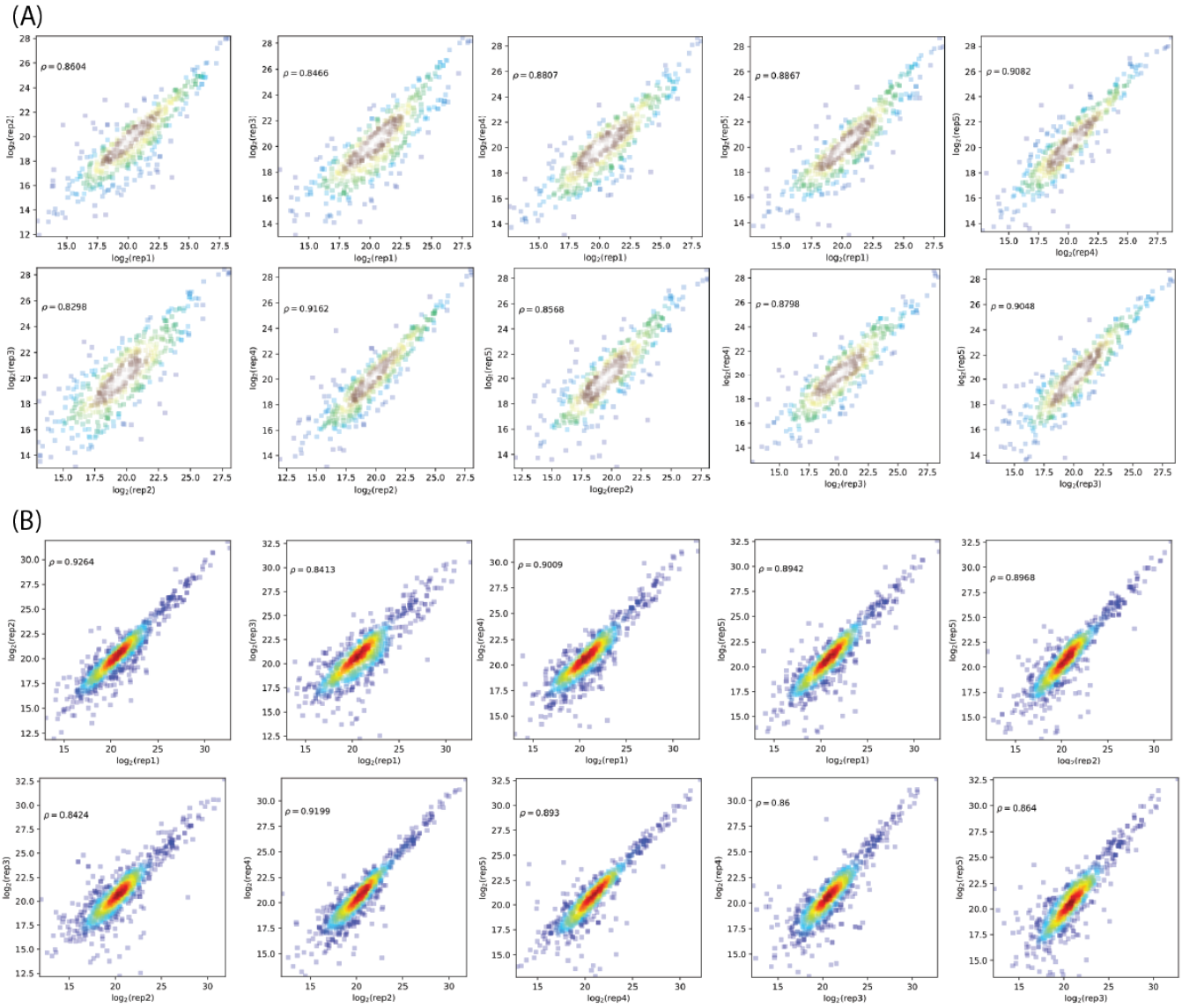

Supplementary Figure 5: Pairwise comparisons between replicates of $\log_2$ transformed phosphopeptide abundances with the same assigned sequence and charge state obtained by sSH2 phosphotyrosine enrichment. (A) Phosphopeptide abundances measured from Raji B cells and (B) Phosphopeptide abundances measured from CD19 CAR T-cells. For each comparison, we used the Pearson's correlation coefficient (denoted ρ) as an estimate of the linear correlation between replicates and thus a measure of reproducibility between replicates.

Supplementary Figure 6: All abundance heat maps for unique phosphopeptides identified by pTyr enrichment after coculture of CD19-CAR T cells and Raji B cells. Included are the protein name, gene name, phosphosite(s), abundance heat maps with significance indicators (if applicable), maximum Ascore, MOWSE score and assigned peptide sequence.

Supplementary Figure 7: All abundance heat maps for unique phosphopeptides identified by TiO_2 phosphopeptide enrichment after coculture of CD19-CAR T cells and Raji B cells. Included are the protein name, gene name, phosphosite(s), abundance heat maps with significance indicators (if applicable), maximum Ascore, MOWSE score and assigned peptide sequence.

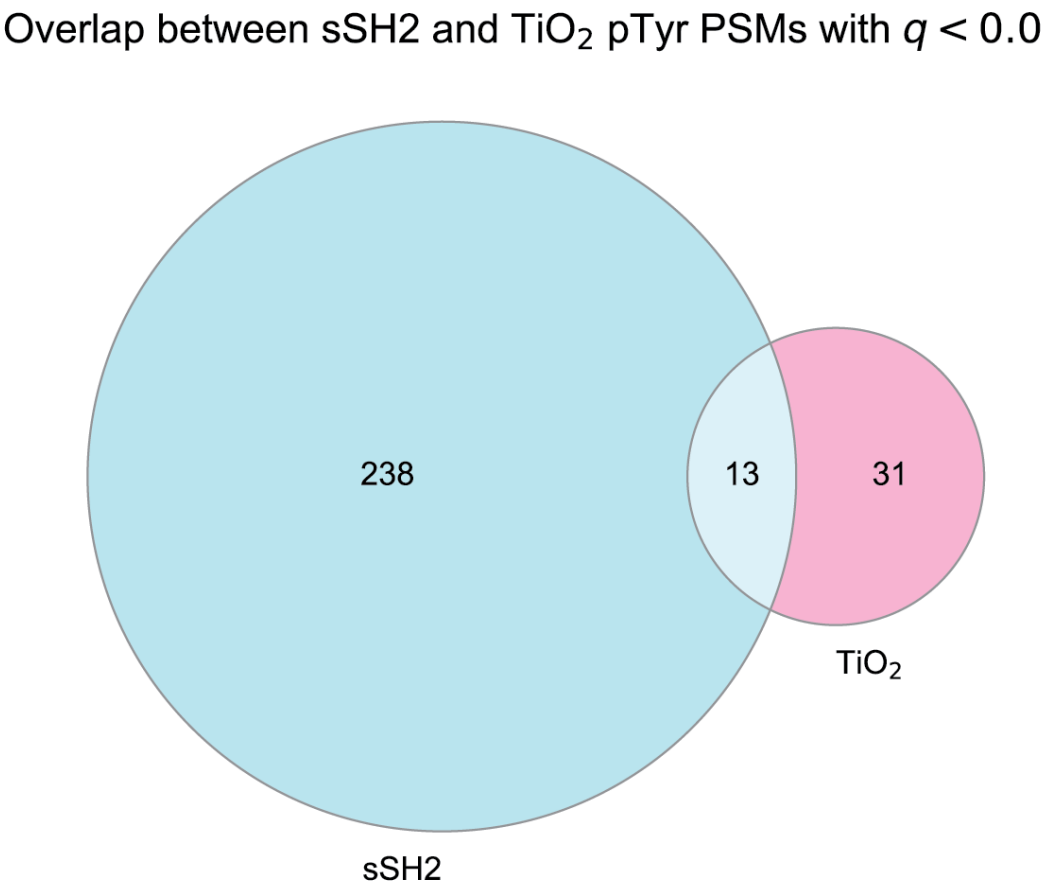

Supplementary Figure 8: Venn diagram showing the overlap between significantly changing sSH2 and TiO_2 pTyr PSMs.

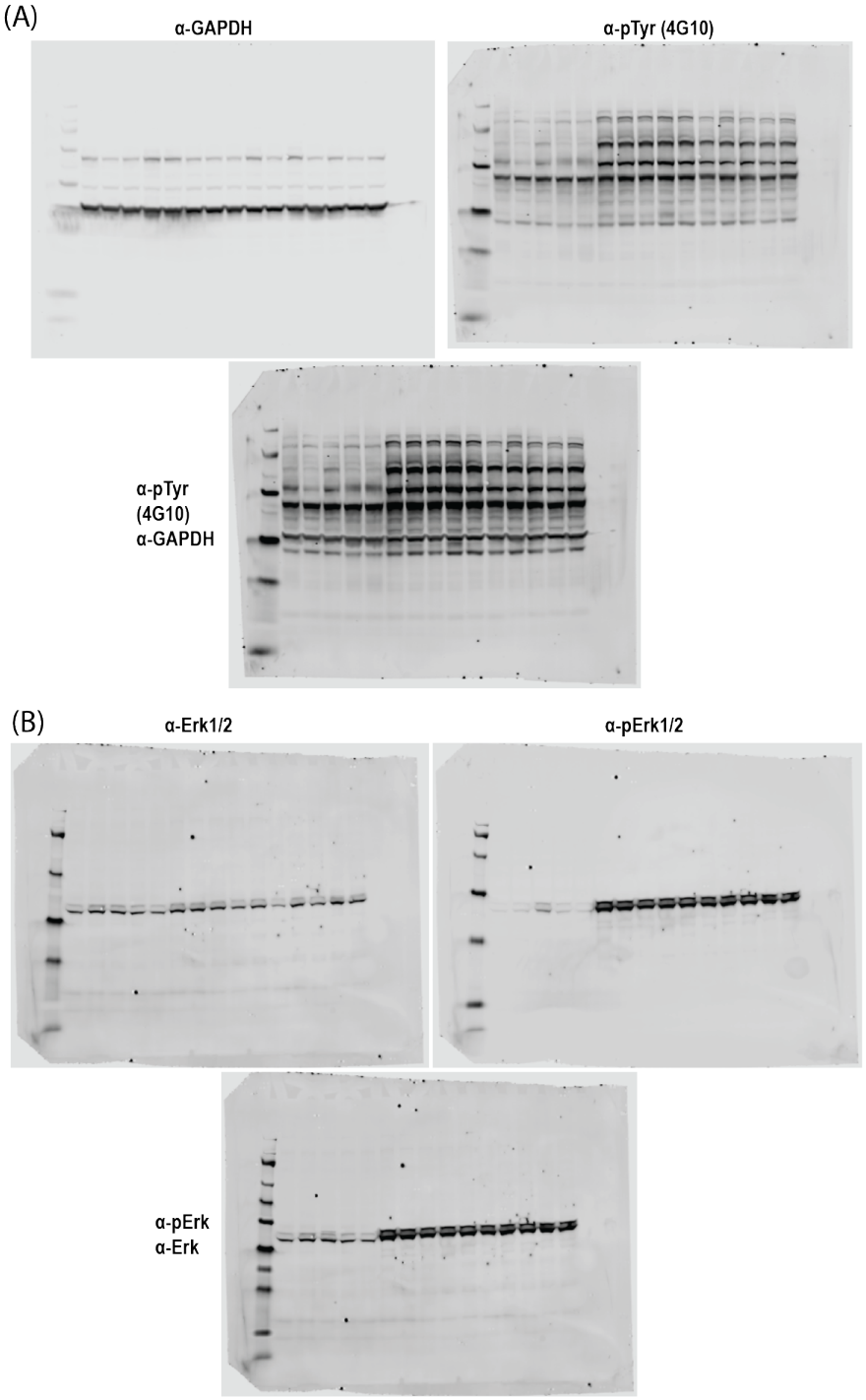

Supplementary Figure 9: Full, uncropped Western blots for (A) α-pTyr (4G10) and (B) α-pErk. Each full blot includes the loading control [α-GAPDH and α-Erk for (A) and (B), respectively], the target, and the merged blots.

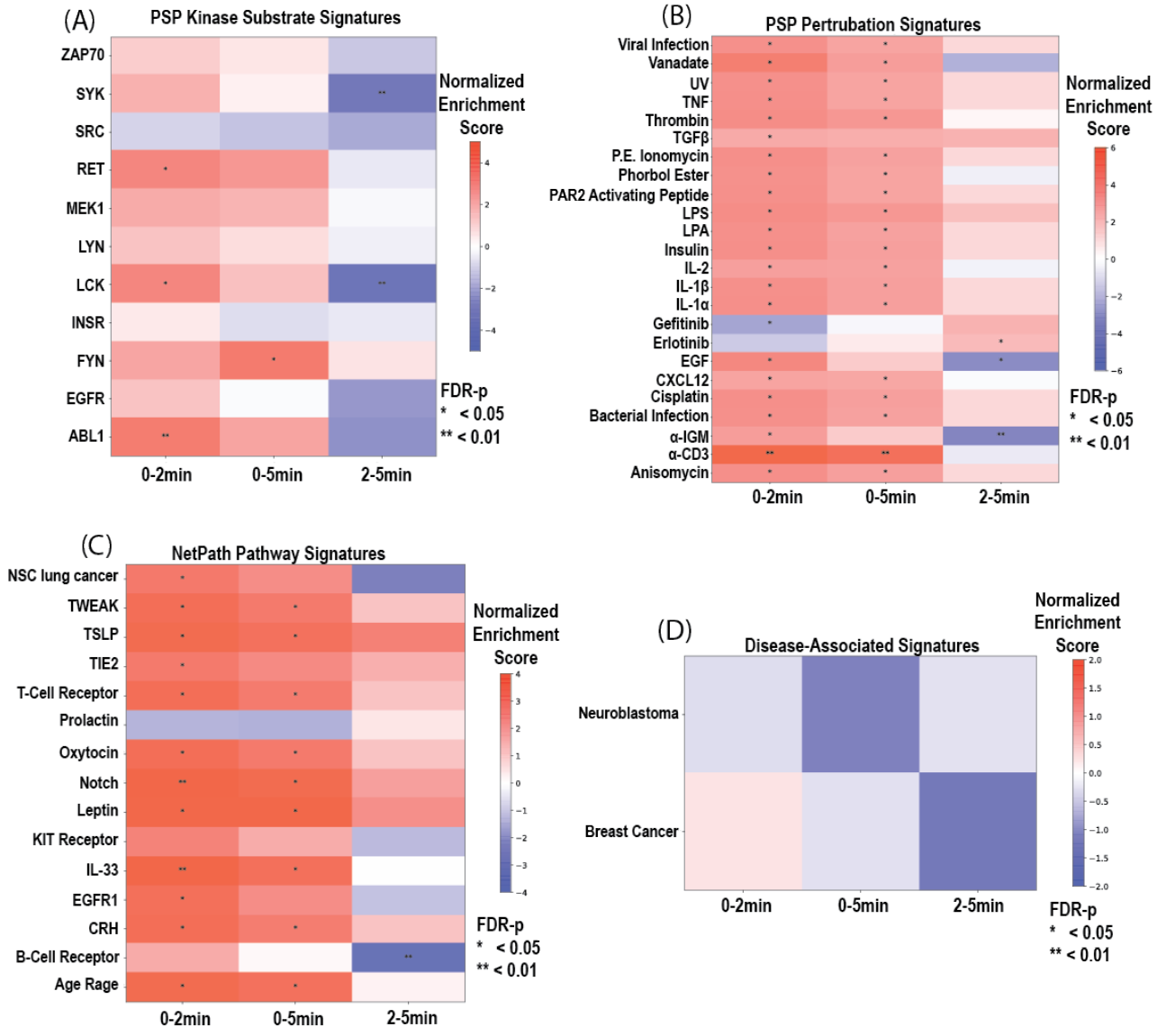

Supplementary Figure 10: PTM-SEA on CD19 CAR T-cell originating phosphopeptides observed in the sSH2 enrichment data. Signature sets (S) in the PTM signature database (PTMsigDB, version 1.9.0) are grouped by (A) PhosphoSitePlus annotated kinase substrate modifications, (B) PhosphoSitePlus annotated modifications that change in response to perturbagens, (C) NetPath annoated modifications associated with a particular signaling pathway, and (D) modifications associated with the progression of a disease. Red colors indicate positive correlations and blue colors indicate negative correlations between signature-associated phosphopeptide abundance changes observed between time points. On each heatmap block, one star ($*$) indicates an $q < 0.05$ and two stars ($**$) indicates an $q < 0.01$.

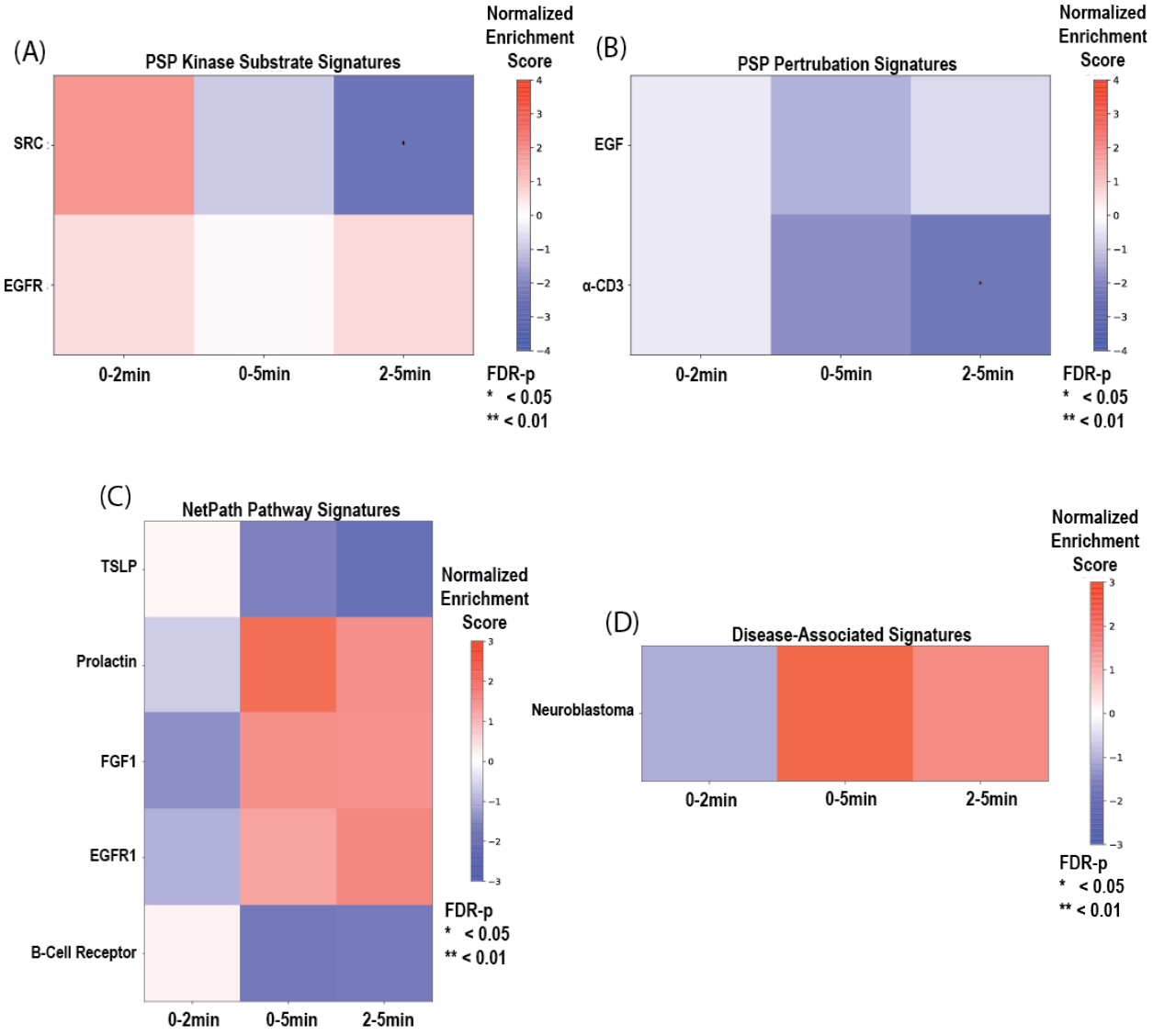

Supplementary Figure 11: PTM-SEA on Raji B-cell originating phosphopeptides observed in the sSH2 enrichment data. Signature sets (S) in the PTM signature database (PTMsigDB, version 1.9.0) are grouped by (A) PhosphoSitePlus annotated kinase substrate modifications, (B) PhosphoSitePlus annotated modifications that change in response to perturbagens, (C) NetPath annoated modifications associated with a particular signaling pathway, and (D) modifications associated with the progression of a disease. Red colors indicate positive correlations and blue colors indicate negative correlations between signature-associated phosphopeptide abundance changes observed between time points. On each heatmap block, one star ($*$) indicates an $q < 0.05$ and two stars ($**$) indicates an $q < 0.01$.

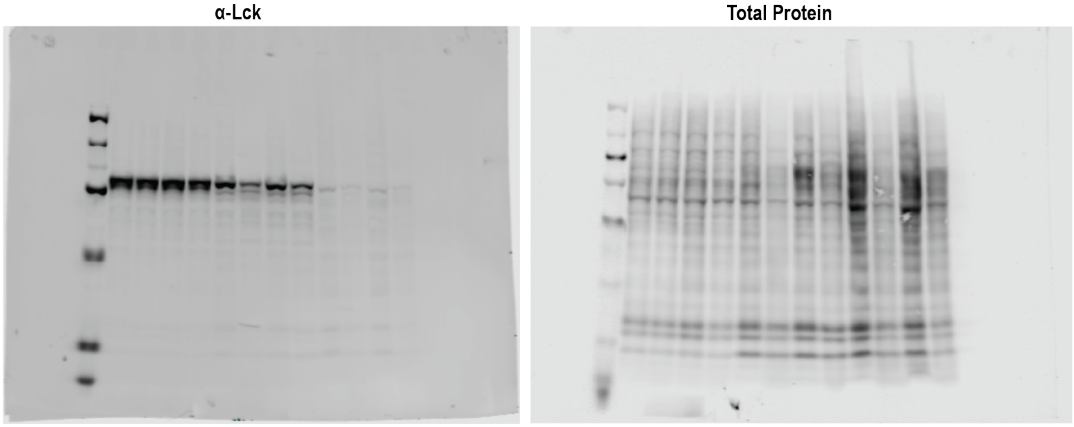

Supplementary Figure 12: Full, uncropped Western blots showing the abundance of Lck protein and total protein abundance in JE6 (Lanes 2-5), CD19-CAR T cells (Lanes 6-9) and Raji B cells (Lanes 10-13).

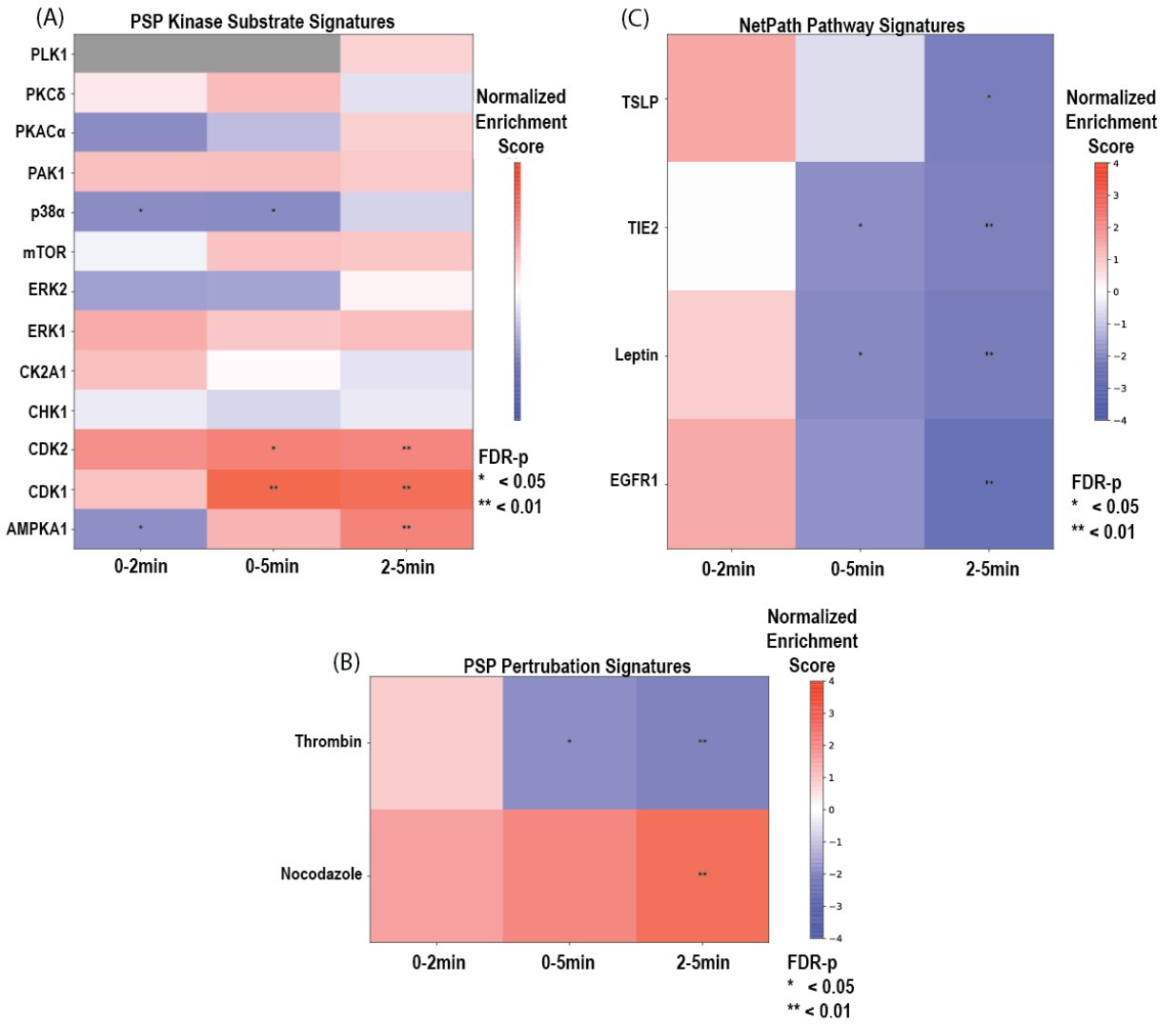

Supplementary Figure 13: PTM-SEA on phosphopeptides originating from Raji B-cell observed in the TiO_2 enrichment data. Signature sets (S) in the PTM signature database (PTMsigDB, version 1.9.0) are grouped by (A) PhosphoSitePlus annotated kinase substrate modifications, (B) PhosphoSitePlus annotated modifications that change in response to perturbagens and (C) NetPath annoated modifications associated with a particular signaling pathway. Red colors indicate positive correlations and blue colors indicate negative correlations between signature-associated phosphopeptide abundance changes observed between time points. On each heat map block, one star ($*$) indicates an $q < 0.05$ and two stars ($**$) indicates an $q < 0.01$.